ADVANCED MATERIALS

vol./vol.; 30 mL). A constant current of typically 1 μA was applied between two platinum electrodes immersed in the solution in two compartments, separated by a glass frit.

X-Ray Crystallography: $C_{24}H_{14}O_{12}S_8$, $M_w = 748.83$, hexagonal, space group $P6_222$ (or $P6_422$), $a = 10.774(1)$ Å, $c = 20.085(2)$ Å, $V = 2119.6(2)$ Å^3, $Z = 3$, crystal size 0.30 mm × 0.15 mm × 0.10 mm, μ(Mo Kα) = 0.697 mm^{-1}. Data were collected using a Rigaku RAXIS-RAPID diffractometer, equipped with an imaging plate area detector (graphite-monochromated Mo Kα radiation, $\lambda = 0.71075$ Å, ω-scan mode (2.0° steps), semi-empirical absorption correction). The structure was solved by direct methods, and refined by full-matrix least-squares against F^2 of all data using the TeXsan program package. Hydrogen atoms, with the exception of those in carboxy groups, were included in the calculated positions, but were not refined. The position of the carboxy hydrogen was determined from the difference Fourier map and isotropically refined. All non-H atoms were refined anisotropically. The refinement converges with $R_1 = 0.032$ for 1340 data ($I > 2\alpha(I)$), $R_w = 0.068$ for all data ($3.63 < \theta < 27.40$), max/min residual electron density 0.28/–0.17 e Å^3.[10]

Received: March 31, 2004
Final version: June 22, 2004

[1] a) *Design of Organic Solids* (Ed.: E. Weber), Topics in Current Chemistry, Vol. 198, Springer, Berlin, Germany **1998**. b) *The Crystal as a Supramolecular Entity* (Ed.: G. R. Desiraju), Wiley, Chichester, UK **1996**. c) *Crystal Design: Structure and Function* (Ed: G. R. Desiraju), Wiley, Chichester, UK **2003**.

[2] a) G. R. Desiraju, *Angew. Chem.* **1995**, *107*, 2541. b) G. R. Desiraju, *Angew. Chem. Int. Ed. Engl.* **1995**, *34*, 2311.

[3] N. Kobayashi, T. Naito, T. Inabe, *Bull. Chem. Soc. Jpn.* **2003**, *76*, 1351.

[4] F. Wudl, *Acc. Chem. Res.* **1984**, *17*, 227.

[5] Crystals with both $P6_222$ and $P6_422$ space groups are thought to be present in the same batch.

[6] The protonated oxygen atoms were determined by the geometry of the COO portion; see [3].

[7] TTF(**I**) is tightly packed in the mellitate double helix by very short O···S contacts of 2.791 Å. The distance is much shorter than the sum of the van der Waals' radii, but such short O···S contacts were observed in the TTF radical salts with oxygen-containing anions; for examples, see a) E. Coronado, J. R. Galan-Mascaros, C. J. Gomez-Garcia, *Dalton* **2000**, 205. b) S. Triki, L. Ouahab, D. Grandjean, *Acta Crystallogr., Sect. C: Cryst. Struct. Commun.* **1993**, *49*, 132.

[8] B. R. Weinberger, E. Ehrenfreund, A. Pron, A. J. Heeger, A. G. MacDiarmid, *J. Chem. Phys.* **1980**, *72*, 4749.

[9] T. Inabe, N. Kobayashi, T. Naito, *J. Phys. IV* **2004**, *114*, 449.

[10] CCDC-225466 contains the supplementary crystallographic data for this paper. These data can be obtained free of charge via www.ccdc.cam.ac.uk/data_request/cif, by emailing data_request@ccdc.cam.ac.uk, or by contacting The Cambridge Crystallographic Data Centre, 12, Union Road, Cambridge CB2 1EZ, UK; fax: +44 1223 336033.

Stable New Sensitizer with Improved Light Harvesting for Nanocrystalline Dye-Sensitized Solar Cells**

By *Peng Wang*, *Shaik M. Zakeeruddin*,* *Jacques E. Moser*, *Robin Humphry-Baker*, *Pascal Comte*, *Viviane Aranyos*, *Anders Hagfeldt*, *Mohammad. K. Nazeeruddin*, and *Michael Grätzel**

Transition metal complexes such as polypyridyl ruthenium(II) have been the subject of extensive electrochemical, photochemical, and photophysical studies stemming from the fact that they exhibit multiple stable oxidation states and attractive excited-state properties. For example, they have been employed as key elements in electrogenerated chemiluminescence,[1–3] organic light-emitting diodes,[4–9] electrochemical and optical sensors,[10–12] molecular wires,[13] molecular machines,[14] photoelectrochemical energy conversion,[15,16] and other fields.[17]

Up to now polypyridyl ruthenium(II) complex based sensitizers[18] have held the efficiency record for solar power conversion in nanocrystalline, dye-sensitized solar cells (DSCs), although recently impressive photovoltaic performance has been demonstrated with metal-free organic dyes.[19,20] Our recent work has revealed that the use of an amphiphilic polypyridyl ruthenium sensitizer, referred to Z-907, is critical to achieve long-term thermal device stability.[21,22] However, the molar extinction coefficient of amphiphilic polypyridyl ruthenium(II) complexes are somewhat lower than the analogous N-719 dye.[23] Thus the development of a new amphiphilic sensitizer with higher molar extinction coefficient and broader spectral response is warranted to achieve better light harvesting and increase the conversion efficiency substantially over 10 %.

4,4′-Di(3-methoxystyryl)-2,2′-bipyridine (dmsbpy) has been employed previously as a ligand for trisbipyridyl-type ruthenium complexes.[24,25] By extending the π-conjugated system of the bipyridine, the metal-to-ligand charge transfer (MLCT)

[*] Dr. S. M. Zakeeruddin, Prof. M. Grätzel, Dr. P. Wang, Dr. J. E. Moser, Dr. R. Humphry-Baker, P. Comte, Dr. M. K. Nazeeruddin
Laboratory for Photonics and Interfaces
Swiss Federal Institute of Technology
Lausanne CH-1015 (Switzerland)
E-mail: shaik.zakeer@epfl.ch; michael.graetzel@epfl.ch
Dr. V. Aranyos, Prof. A. Hagfeldt
Department of Physical Chemistry
University of Uppsala
Box 532, SE-75121, Uppsala (Sweden)

[**] The present work is supported by the Swiss Science Foundation, the Swiss Federal Office for Energy (OFEN), and the European Office of U.S. Air Force under Contract No. F61775-00-C0003. V. A. and A. H. would like to thank the Swedish Foundation for Strategic Environmental Research (MISTRA) and the Swedish National Energy Administration for financial support. We thank M. Jirousek, R. Charvet, P. Liska, and T. Sekiguchi for helpful discussions.

  DOI: 10.1002/adma.200400039

transition of $Ru(dmsbpy)_3^{2+}$ is red-shifted and shows a higher molar extinction coefficient when compared with $Ru(bpy)_3^{2+}$. We report on the use of this ligand in a heteroleptic analogue of the Z-907 sensitizer. It will be shown that introducing this ligand enhances the harvesting of solar light, making this new sensitizer a promising candidate for improving the conversion efficiencies of dye-sensitized solar cells.

The molecular structure of $Ru(dcbpy)(dmsbpy)(NCS)_2$ (dcbpy = 4,4′-dicarboxylic acid-2,2′-bipyridine), referred to Z-910, is shown in Figure 1. This new heteroleptic dye was synthesized according to a recently developed one-pot synthetic procedure[21] and characterized by ^1H NMR, elemental

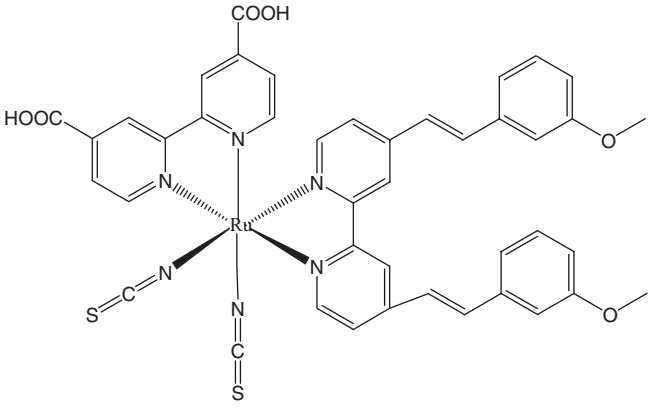

Figure 1. Molecular structure of Z-910 dye.

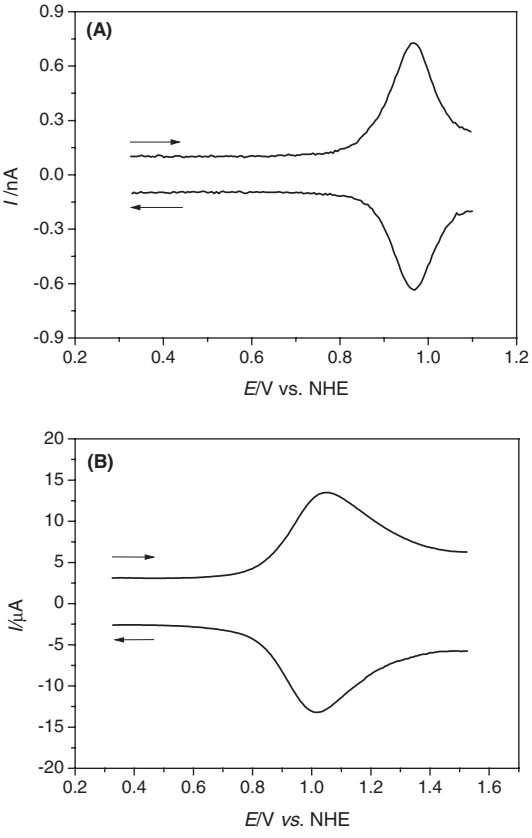

Figure 2. Square-wave voltammograms of A) a Pt ultramicroelectrode in DMF solution containing Z-910 and B) a nanocrystalline TiO_2 electrode anchored with Z-910 in DMF. Supporting electrolyte: 0.1 M $TBAPF_6$. Potential step increment: 10 mV; frequency: 25 Hz.

analysis, voltammetry, and Fourier-transform infrared (FTIR) spectroscopy, as well as electronic absorption and emission spectroscopy.

Sensitization of TiO_2 nanocrystalline electrodes to visible light relies on the fact that the excited state of a dye is a stronger reductant than in the ground state. Knowledge of the formal redox potential of the excited state [$\phi^0(S^+/S^*)$] of a dye relative to the conduction band energy level of TiO_2 semiconductor allows prior determination of the direction of current flow.[26–28] An approximate $\phi^0(S^+/S^*)$ value of a dye can be extracted from the formal potential of the ground state [$\phi^0(S^+/S)$] and its excitation energy (E_{0-0}), according to Equation 1 (where F is the Faraday constant), where the values are derived from electrochemical and spectroscopic measurements.

$$\phi^0(S^+/S^*) = \phi^0(S^+/S) - E_{0-0}/F \quad (1)$$

Accurate determination of redox potential was achieved via square-wave voltammetry with inherently high analytical sensitivity and strong immunity to capacitive effects.[29] As presented in Figure 2A, both anodic and cathodic peaks arise at 0.97 V versus NHE (normal hydrogen electrode) for the Z-910 dye in dimethylformamide (DMF) solution, which was measured with a Pt ultramicroelectrode, which was insensitive to the solution ohmic drop since only a very small current passed through the electrolytic cell. Figure 2B shows square-wave voltammograms of Z-910 anchored on the TiO_2 nanocrystalline film. The 40 mV peak–peak separation could be caused by the uncompensated ohmic drop in the electrolyte solution, slow direct electron transfer between the conducting glass and the Z-910 dye anchored onto the TiO_2 surface, or slow electrostatic charge compensation during the redox process. The formal redox potential of anchored Z-910 is calculated to be 1.03 V versus NHE by averaging the anodic and cathodic peak potentials. The 60 mV positive shift after anchoring Z-910 onto TiO_2 is indicative of an electron density decrease in the ruthenium center due to electronic coupling between the highest occupied molecular orbital (HOMO) of the Z-910 dye and surface titanium ions through the carboxylate bridge.

The MLCT absorption bands of the Z-910 dye presented in Figure 3A have two maxima at 410 and 543 nm, which are about 20 nm red-shifted compared to those of Z-907 and its analogues.[23] The molar extinction coefficients of these two bands are 17.01×10^3 and 16.85×10^3 $M^{-1}\,cm^{-1}$. These are significantly higher than the corresponding values for the Z-907 analogues and standard N-719 dye.[23] In addition, the improved light-harvesting by extending the π-conjugated system can be clearly seen from Figure 3B, which presents the visible

ADVANCED MATERIALS

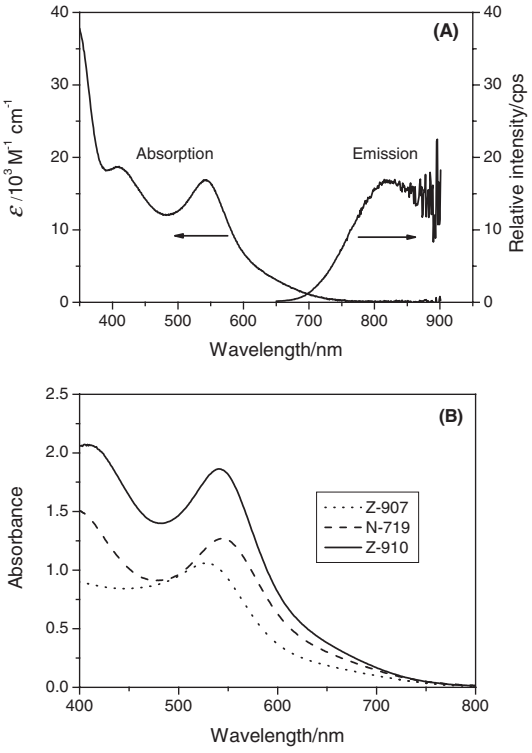

Figure 3. A) Electronic absorption and emission spectra of Z-910 dye in acetonitrile. B) Absorption spectra of Z-910, N-719, and Z-907 anchored on the 8 μm thickness transparent nanocrystalline TiO_2 film.

region absorption spectra of Z-910, N-719, and Z-907 anchored on the 8 μm thick transparent nanocrystalline TiO_2 film.

Excitation of the low energy MLCT transition of the Z-910 dye in acetonitrile produces an emission centered at 818 nm, shown in Figure 3A. The emission spectrum was further analyzed by applying a Gaussian reconvolution method, which enabled determination of the integral under the emission peak, devoid of Raman and other instrumental artefacts. E_{0-0} transition energy was estimated to be 1.7 eV, and thus $\phi^0(S^+/S^*)$ of Z-910 was calculated to be –0.73 V versus NHE. The more negative $\phi^0(S^+/S^*)$ relative to the conduction band edge of TiO_2 ensures the thermodynamic driving force of electron injection.[16] Additionally, the excited-state lifetime of Z-910 in DMF was determined by transient absorbance measurements at 600 nm to be 31 ns, which allows efficient electron injection from the excited-state dye molecules before deactivation, as the injection process occurs on a time scale of femtoseconds or picoseconds.[16,18]

An attenuated total reflectance FTIR (ATR-FTIR) spectrum of Z-910 measured as powder shows the most prominent bands at 2099 cm^{-1} (–NCS), 1717 cm^{-1} (C=O), and 1240 cm^{-1} (C–O). The spectrum of Z-910 anchored on TiO_2 film (Fig. 4) clearly shows the bands at 1604 and 1383 cm^{-1} for the asymmetric and symmetric stretching modes of the carboxylate group, indicating that the two carboxylic acid groups are deprotonated and are involved in the adsorption of the dye on

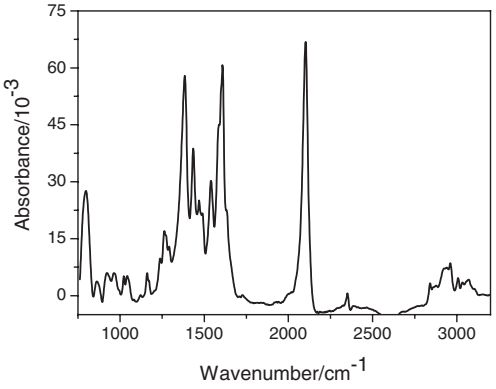

Figure 4. ATR-FTIR spectra for a 4 μm mesoporous TiO_2 film coated with Z-910 dye. A TiO_2 reference film heated at 500 °C to remove surface-adsorbed water has been subtracted for clarity of presentation.

the surface of TiO_2. From these ATR-FTIR data one infers that the dye is anchored on the surface though the carboxylate groups via a bidentate chelation or a bridging of surface titanium ions rather than an ester-type linkage.[30] The –NCS group absorption remains at 2099 cm^{-1}, indicating that the NCS coordinated to the ruthenium center through the N atom is unaffected by the adsorption process. The other peaks observed at 2957 and 2840 cm^{-1} correspond to the asymmetric and symmetric stretching modes of the CH_3 unit, while sp^2 C–H stretching mode is observed at 3065 cm^{-1}. The sharp peaks located at 1539 and 1432 cm^{-1} arise from bipyridyl ring modes.

Electron injection from the photoexcited sensitizer is followed by recapture of the electrons trapped in the TiO_2 film (e_{cb}^-) by the oxidized sensitizer or by regeneration of the sensitizer via electron donation from iodide ions. Since the kinetic competition between these controls, to a large extent, the photon-to-current conversion efficiency of the photovoltaic device, nanosecond time-resolved laser experiments[31–33] were designed to scrutinize the kinetics of the recombination from the conduction band of TiO_2 to the oxidized state of dye molecules (S^+), and that of the interception of the oxidized sensitizer by iodide in the electrolyte.

Transient absorbance signals obtained at probe wavelengths larger than 620 nm are characteristic of the ligand-to-metal charge transition (LMCT) of a polypyridyl ruthenium(III) complex with thiocyanate ligand.[34,35] In the absence of a redox mediator (Fig. 5, trace a), the decay of the absorption signal recorded at 650 nm reflects the dynamics of the recombination of injected electrons with the oxidized state (S^+) of the Z-910 molecules, produced by electron injection from the photoexcited dye into the semiconductor film. The pulsed laser intensity was kept at a low level (fluence: ~40 μJ cm^{-2} per pulse at the sample) to ensure that an average of less than one e_{cb}^-/S^+ charge-separated pair is produced for every nanocrystalline TiO_2 particle. These experimental conditions are believed to be comparable to those prevailing in the functioning photovoltaic device. The kinetics of the S^+ transient absor-

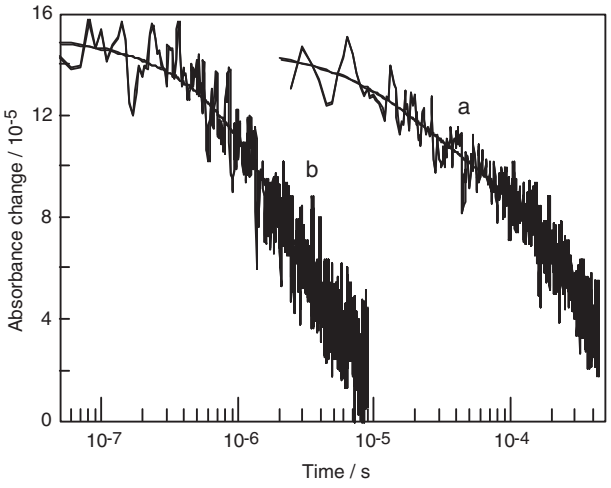

Figure 5. Transient absorbance decay kinetics of the oxidized state of Z-910 anchored on a nanocrystalline TiO_2 film a) in pure acetonitrile/valeronitrile (volume ratio: 3:1) solvent mixture and b) in the presence of the electrolyte used for device A. Absorbance changes were measured at a probe wavelength of 650 nm, employing 543 nm laser excitation (5 ns full width at half maximum pulse duration, 40 μJ cm^{-2} pulse fluence).

bance decay could be fitted by a double exponential with a typical half-reaction time ($t_{1/2}$) of 180 μs. In the presence of the electrolyte containing iodide, the decay of the oxidized dye signal was significantly accelerated, with $t_{1/2} = 2$ μs, showing that recombination is indeed efficiently intercepted by the redox mediator (Fig. 5, trace b). In such conditions, the fraction of the initial S^+ species population that can undergo recombination with conduction band electrons is estimated to be lower than 5 %.

A screen-printed double layer of TiO_2 particles was used as the photoanode. A 10 μm thick film of 20 nm sized TiO_2 particles was first printed on the fluorine-doped SnO_2 conducting glass electrode, and then coated by a 4 μm thick second layer of 400 nm sized light-scattering anatase particles. A detailed fabrication procedure for the nanocrystalline TiO_2 photoanodes and the assembly, as well as photoelectrochemical characterization of complete, hot-melt sealed cells has been described elsewhere.[36] The electrolyte used for device A contained 0.6 M 1-propyl-3-methylimidazolium iodide (PMII), 30 mM I_2, 0.13 M guanidinium thiocyanate, and 0.5 M 4-*tert*-butylpyridine in the mixture of acetonitrile and valeronitrile (volume ratio: 3:1). The TiO_2 electrodes were immersed at room temperature for 12 h in a solution of 300 μM Z-910 and 300 μM chenodeoxycholic acid in acetonitrile and *tert*-butanol (volume ratio: 1:1). For stability tests, the electrolyte was composed of 0.6 M PMII, 0.1 M I_2, and 0.5 M *N*-methylbenzimidazole in 3-methoxypropionitrile, and the corresponding device with the Z-910 dye alone is denoted as device B.

The photocurrent action spectrum of device A with Z-910 as sensitizer is shown in Figure 6A. The incident photon-to-current conversion efficiency (IPCE) exceeds 80 % in the spectral range 470–620 nm, reaching its maximum of 87 % at

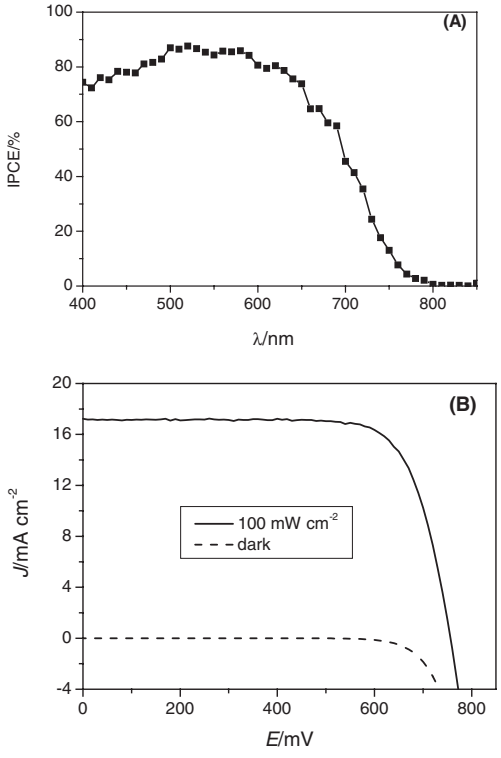

Figure 6. A) Photocurrent action spectrum of device A. B) Current density–voltage characteristics of device A under AM 1.5 sunlight (100 mW cm^{-2}) illumination and in the dark. Cell active area: 0.158 cm^2. Regions outside the active area are completely masked with black plastic to avoid the diffusive light.

520 nm. Considering the light absorption and scattering loss by the conducting glass, the maximum efficiency for absorbed photon-to-current conversion efficiency is practically unity over this spectral range. From the overlap integral of this curve with the standard global air mass (AM) 1.5 solar emission spectrum, a short-circuit photocurrent density (J_{sc}) of 17.2 mA cm^{-2} is calculated, which is in excellent agreement with the measured photocurrent. As shown in Figure 6B, the short-circuit photocurrent density (J_{sc}), open-circuit photovoltage (V_{oc}), and fill factor (*ff*) of device A with Z-910 dye under AM 1.5 full sunlight are 17.2 mA cm^{-2}, 777 mV, and 0.764, respectively, yielding an overall conversion efficiency (η) of 10.2 %. At various lower incident-light intensities, overall power conversion efficiencies are also over 10.2 %. With the double layer film (total thickness of 14 μm) and electrolyte used here, the power conversion efficiencies of N-719 and Z-907 dyes are 7 % less efficient than Z-910.

Due to the difficulty in sealing a highly volatile solvent for thermal tests, a 3-methoxypropionitrile-based electrolyte was used for the stability test of this new sensitizer under moderate thermal stress and visible-light soaking. The advantage of using 3-methoxypropionitrile lies in its high boiling point, low volatility, non-toxicity and good photochemical stability, making it viable for practical application. The photovoltaic parameters (J_{sc}, V_{oc}, *ff*, and η) of device B are 14.8 mA cm^{-2},

ADVANCED MATERIALS

696 mV, 0.695, and 7.2 %, respectively. The cells covered with a 50 μm thick polyester film (Preservation Equipment Ltd, UK) as a UV cut-off filter (up to 400 nm) were irradiated at open circuit under a Suntest CPS plus lamp (ATLAS GmbH, 100 mW cm^{-2}, 55 °C). As shown in Figure 7, all parameters of the device are rather stable during 1000 h accelerating tests. It should be noted that under this condition the new sensitizer showed similar stability but higher efficiency compared with Z-907 dye.

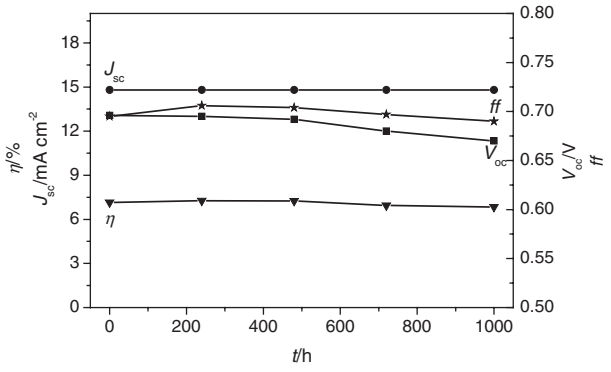

Figure 7. Detailed photovoltaic parameters of device B during successive one sun visible-light soaking at 55 °C.

In conclusion, a new heteroleptic polypyridyl ruthenium complex with a high molar extinction coefficient has been synthesized and demonstrated as a highly efficient, stable sensitizer for nanocrystalline solar cells. For a newly developed dye, the achievement of 10.2 % power conversion efficiency is very encouraging. Enhancing the molar extinction coefficient of sensitizers has been demonstrated to be an elegant strategy to improve the photovoltaic performance of dye-sensitized solar cells. Work is in progress to optimize the cell parameters to take full advantage of the potential of this new and promising sensitizer.

Experimental

The synthesis of Z-910 was performed according to the procedure reported in our previous paper [21]. In a typical one-pot synthesis of Z-910, $[RuCl_2(p\text{-cymene})]_2$ (0.15 g, 0.245 mmol) was dissolved in DMF (50 mL) and dmsbpy (0.206 g, 0.49 mmol) was added to this solution. The reaction mixture was heated to 60 °C under nitrogen for 4 h with constant stirring. dcbpy (0.12 g, 0.49 mmol) was added to this reaction flask and refluxed for 4 h. Finally, excess of NH_4NCS (13 mmol) was added to the reaction mixture and refluxed for another 4 h. The reaction mixture was cooled to room temperature and the solvent was removed by using a rotary evaporator under vacuum. Water was added to the flask and the insoluble solid was collected on a sintered glass crucible by suction filtration. The crude was dissolved in a basic methanolic solution and purified by passing through a Sephadex LH-20 column with methanol as an eluent. After collecting the main band and evaporating the solvent, the resultant solid was redissolved in water. Lowering the pH to 3.1 by titration with dilute nitric acid produced Z-910 as a precipitate. The final product was washed thoroughly with water and dried under vacuum. ^{1}H NMR (δ_H/ppm in CD_3OD with NaOD): 9.4 (d, 1H), 9.2 (d, 1H), 8. 9 (s, 1H), 8.8 (s, 1H), 8.3 (s, 1H), 8.15 (s, 1H), 7.9 (d, 1H), 7.80 (d, 1H), 7.7 to 6.9 (m, 16H), 4.1 (s, 3H), 4.0 (s, 3H). Anal. Calc. for $RuC_{42}H_{34}N_6O_7S_2$: C, 56.0; H, 3.78; N, 9.34 %. Found: C, 55.22; H, 3. 97; N, 9.39 %.

A computer-controlled Autolab P20 electrochemical workstation (Eco Chimie, Netherlands) was used for square-wave voltammetric measurements in combination with a conventional three-electrode, one-compartment electrochemical cell. A Pt foil electrode and an Ag/AgCl/KCl_{sat} electrode were used as counter and reference electrodes, respectively. Due to the possible liquid junction potential, the used reference electrode was frequently calibrated by measuring the redox potential of ferrocene. The redox potential values versus calibrated Ag/AgCl/KCl_{sat} were converted to those versus NHE. For the electrochemical study of Z-910 dissolved in DMF, a Pt ultramicroelectrode with a radius of 5.0 μm (Bioanalytical Systems, Inc., USA) was used as working electrode. A dye-coated photoanode was used as working electrode to study the electrochemical behavior of Z-910 on the nanocrystalline TiO_2 film.

Received: December 1, 2003
Final version: April 21, 2004

[1] N. E. Tokel, A. J. Bard, *J. Am. Chem. Soc.* **1972**, *94*, 2862.
[2] M. M. Richter, A. J. Bard, W. Kim, R. H. Schmehl, *Anal. Chem.* **1998**, *70*, 310.
[3] W. Miao, J.-P. Choi, A. J. Bard, *J. Am. Chem. Soc.* **2002**, *124*, 14 478.
[4] S. Welter, K. Brunner, J. W. Hofstraat, L. De Cola, *Nature* **2003**, *421*, 54.
[5] J. Slinker, D. Bernards, P. L. Houston, H. D. Abruña, S. Bernhard, G. G. Malliaras, *Chem. Commun.* **2003**, 2392.
[6] G. Kalyuzhny, M. Buda, J. McNeill, P. Barbara, A. J. Bard, *J. Am. Chem. Soc.* **2003**, *125*, 6272.
[7] H. Rudmann, S. Shimada, M. F. Rubner, *J. Am. Chem. Soc.* **2002**, *124*, 4918.
[8] X. Gong, P. K. Ng, W. K. Chan, *Adv. Mater.* **1998**, *10*, 1337.
[9] K. M. Maness, R. H. Terrill, T. J. Meyer, R. W. Murray, R. M. Wightman, *J. Am. Chem. Soc.* **1996**, *118*, 10 609.
[10] T. G. Drummond, M. G. Hill, J. K. Barton, *Nat. Biotechnol.* **2003**, *21*, 1192.
[11] P. D. Beer, *Acc. Chem. Res.* **1998**, *31*, 71.
[12] Y. Z. Hu, Q. Xiang, R. P. Thummel, *Inorg. Chem.* **2002**, *41*, 3423.
[13] F. Barigelletti, L. Flamigni, *Chem. Soc. Rev.* **2000**, *29*, 1.
[14] R. Ballardini, V. Balzani, A. Credi, M. T. Gandolfi, M. Venturi, *Acc. Chem. Res.* **2001**, *34*, 445.
[15] V. Balzani, S. Campagna, G. Denti, A. Juris, S. Serroni, M. Venturi, *Acc. Chem. Res.* **1998**, *31*, 26.
[16] M. Grätzel, *Nature* **2001**, *414*, 338.
[17] J.-P. Sauvage, J.-P. Collin, J.-C. Chambron, S. Guillerez, C. Coudret, V. Balzani, F. Barigelletti, L. De Cola, L. Flamigni, *Chem. Rev.* **1994**, *94*, 993.
[18] M. Grätzel, *J. Photochem. Photobiol. C* **2003**, *4*, 145.
[19] K. Hara, M. Kurashige, Y. Dan-oh, C. Kasada, A. Shinpo, S. Suga, K. Sayama, H. Arakawa, *New J. Chem.* **2003**, *27*, 783.
[20] T. Horiuchi, H. Miura, S. Uchida, *Chem. Commun.* **2003**, 3036.
[21] P. Wang, S. M. Zakeeruddin, J. E. Moser, M. K. Nazeeruddin, T. Sekiguchi, M. Grätzel, *Nat. Mater.* **2003**, *2*, 402.
[22] P. Wang, S. M. Zakeeruddin, R. Humphry-Baker, J. E. Moser, M. Grätzel, *Adv. Mater.* **2003**, *15*, 2101.
[23] S. M. Zakeeruddin, M. K. Nazeeruddin, R. Humphry-Baker, P. Péchy, P. Quagliotto, C. Barolo, G. Viscard, M. Grätzel, *Langmuir* **2002**, *18*, 952.
[24] V. Aranyos, J. Hjelm, A. Hagfeldt, H. Grennberg, *J. Chem. Soc. Dalton Trans.* **2001**, 1319.
[25] V. Aranyos, J. Hjelm, A. Hagfeldt, H. Grennberg, *J. Chem. Soc. Dalton Trans.* **2003**, 1280.
[26] P. Qu, G. J. Meyer, in *Electron Transfer in Chemistry*, Vol. IV (Ed: V. Balzani), Wiley-VCH, Weinheim, Germany **2001**.

[27] M. Grätzel, J. E. Moser, in *Electron Transfer in Chemistry*, Vol. V (Ed: V. Balzani), Wiley-VCH, Weinheim, Germany **2001**.
[28] A. J. Bard, M. Stratmann, *Encyclopedia of Electrochemistry*, Vol. 6, Wiley-VCH, Weinheim, Germany **2002**.
[29] J. Osteryoung, J. J. O'Dea, in *Electroanalytical Chemistry*, Vol. 14 (Ed: A. J. Bard), Marcel Dekker, New York **1986**.
[30] V. Shklover, Y. E. Ovehinnikov, L. S. Braginsky, S. M. Zakeeruddin, M. Grätzel, *Chem. Mater.* **1998**, *10*, 2533.
[31] S. Pelet, J. E. Moser, M. Grätzel, *J. Phys. Chem. B* **2000**, *104*, 1791.
[32] P. Wang, S. M. Zakeeruddin, J. E. Moser, M. Grätzel, *J. Phys. Chem. B* **2003**, *107*, 13 280.
[33] S. A. Haque, E. Palomares, H. M. Upadhyaya, L. Otley, R. J. Potter, A. B. Holmes, J. R. Durrant, *Chem. Commun.* **2003**, 3008.
[34] Y. Tachibana, J. E. Moser, M. Grätzel, D. R. Klug, J. R. Durrant, *J. Phys. Chem.* **1996**, *100*, 20 056.
[35] J. E. Moser, D. Noukakis, U. Bach, Y. Tachibana, D. R. Klug, J. R. Durrant, R. Humphry-Baker, M. Grätzel, *J. Phys. Chem. B* **1998**, *102*, 3649.
[36] P. Wang, S. M. Zakeeruddin, P. Comte, R. Charvet, R. Humphry-Baker, M. Grätzel, *J. Phys. Chem. B* **2003**, *107*, 14 336.

Porous Silicon Photonic Crystals as Encoded Microcarriers**

By *Shawn O. Meade*, *Myeong Sik Yoon*, *Kyo Han Ahn*, and *Michael J. Sailor**

Multiplexed assays are used to study genomes for variation and function, to identify candidate drugs, and in a variety of other applications in which a large number of parallel experiments must be performed in a short period of time.[1,2] Beads or particles containing many independent codes are useful for these applications, and various encoding schemes have been proposed, involving for example quantum dots, fluorescent molecules, metal rods, and porous silicon photonic crystals.[3–8] In the present work, a method of preparing one-dimensional photonic crystals with multiple peaks in their optical reflectivity spectrum is described. The technique involves electrochemically etching a composite current–time waveform into a silicon wafer. The porous nanostructure that results exhibits an optical reflectivity spectrum that represents the Fourier transform of the porosity gradient defined in the electrochemical etch. The resulting spectral peaks can be used as an optical barcode, and the possibility of generating over one million unique codes is demonstrated.

The algorithm used to prepare an encoded porous silicon film is summarized in Figure 1. Bovard et al.[9] first proposed a similar concept in the design of optical filters. The method involves creating a refractive index variation in a material whose spatial distribution consists of the sum of several sine waves. The optical spectrum (intensity versus frequency) that results from such a structure represents the Fourier transform of the spatial distribution of refractive index (refractive index versus distance) in the material. Berger et al.[10] first demonstrated the application of this concept to the design of rugate filters from porous silicon. The waveform used in the present work involves a superposition of n sine waves of different

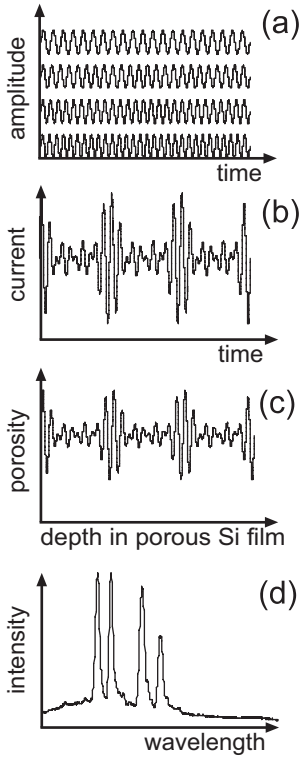

Figure 1. Representation of the encoding method used in this work. In this example, four sine waves with different frequencies (a) are summed to generate a composite waveform (b) that is then converted into a current-time waveform in the computer-controlled current source, etching a porosity–depth profile into the Si wafer (c). The resulting optical reflectivity spectrum (d) displays the four frequency components of the original four sine waves as separate spectral peaks. Representing the Fourier transform of the composite waveform, the wavelength and intensity of each peak in the spectrum is determined by the frequency and amplitude, respectively, of its corresponding sine component.

[*] Prof. M. J. Sailor, S. O. Meade
Department of Chemistry and Biochemistry
The University of California
San Diego, 9500 Gillman Drive, La Jolla
CA 92039-0358 (USA)
E-mail: msailor@ucsd.edu
M. S. Yoon, Prof. K. H. Ahn
Department of Chemistry and
Center for Integrated Molecular Systems
Division of Molecular and Life Science
Pohang University of Science and Technology
San 31 Hyoja-dong, Pohang 790–784 (Republic of Korea)

[**] The authors acknowledge financial support from TREX industries, inc., the National Institutes of Health and the Air Force Office of Scientific Research (Grant# F49620-02-1-0288). Supporting Information for this article is available online from Wiley InterScience or from the author.

 DOI: 10.1002/adma.200400713